

# Dehydration behavior and structural characterization of the GW275919X monohydrate

Haijian (Jim) Zhu\*

Strategic Technologies, GlaxoSmithKline Inc., Five Moore Drive, Research Triangle Park, NC 27709, United States

Received 31 January 2005; received in revised form 11 October 2005; accepted 25 January 2006

Available online 6 March 2006

## Abstract

GW275919X, a central muscle relaxant for the treatment of lower back pain, exists in a monohydrate. Knowledge of the solid state dehydration behavior and the crystal structure is essential for determining its relative physical stability. Thermal analysis and hot-stage powder X-ray diffraction were used to study the solid state phase transformation during the dehydration process. Crystal structure was determined by single crystal X-ray analysis. Molecular modeling with Cerius<sup>2</sup> software was used to visualize the hydrate crystal structure and to construct the molecular packing and hydrogen bond diagram. Morphology prediction was performed using the BFDH calculation. Crystallographic data: monoclinic, space group,  $P21/c$ ,  $a$  (Å) = 14.3734,  $b$  (Å) = 5.0336,  $c$  (Å) = 15.4633 and  $\beta = 105.11^\circ$ . Water molecules in the hydrate crystal of GW275919X are involved in the hydrogen bonds and these hydrogen bonds contribute to the coherence of the crystal structure. The longest dimension of the predicted morphology is in the  $b$ -direction, which would correspond to the needle axis of the experimental crystals.

© 2006 Elsevier B.V. All rights reserved.

**Keywords:** GW275919 monohydrate; Dehydration; Hydration; Thermal analysis; PXRD; Modeling

## 1. Introduction

A larger number of drugs crystallize to form hydrates (Byrn, 1982). Knowledge of the relationship between dehydration behavior of a hydrate and its crystal structure is essential for determining the relative physical stability (Hirsch et al., 1978; Forbes et al., 1992; Agbada and York, 1994; Ojala et al., 1996; Zhu et al., 1996, 2001a).

GW275919X (Fig. 1) is a central muscle relaxant for the treatment of lower back pain. Six crystal forms, including three anhydrous polymorphs (Forms I, II and III), a monohydrate and a DMF solvate and a DMA solvate have been identified through crystallization screening (Zhu and Sacchetti, 2001). In this study, the monohydrate of GW275919X was characterized and solid state phase transformation during the dehydration process was studied by thermal analysis and hot-stage powder X-ray diffraction. Crystal structure of the monohydrate was determined by single crystal X-ray analysis. Molecular modeling with Cerius<sup>2</sup>

software was used to visualize the hydrate crystal structure and to construct the molecular packing and hydrogen bond diagram. The preliminary results of this study were presented previously in a poster presentation (Zhu et al., 2001b).

## 2. Materials and methods

### 2.1. Materials

GW275919X was manufactured at GlaxoSmithKline Inc., Research Triangle Park, NC. All other materials were reagent grade or better and used without further purification.

### 2.2. Preparation of single crystals and structure determination of GW275919X monohydrate

The single crystal of GW275919X monohydrate was prepared by gradually cooling a saturated acetone:water (2:1) solution of GW275919X from 60 °C to room temperature. Wet crystals were submitted to the X-ray Crystallographic Facility at the Chemistry Department, University of North Carolina, Chapel Hill. The  $2\theta$  and intensity data were collected at  $-100^\circ\text{C}$  using a Bruker SMART diffractometer. Unit cell dimensions

\* Present address: Forest Laboratories, Inc., 220 Sea Lane, Farmingdale, NY 11735, United States. Tel.: +1 631 501 5358; fax: +1 631 501 5400.

E-mail address: [jim.zhu@frx.com](mailto:jim.zhu@frx.com).

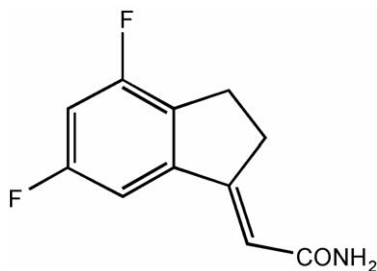


Fig. 1. Molecular structure of GW275919X.

were obtained from 6683 reflections. Structure solution and refinement was based on 2466 unique and significant reflections ( $R_f = 0.062$  and  $R_w = 0.064$ ). The program used for data reduction and analysis has been described (Gabe et al., 1989). UNC single crystal structure results were reported to the authors in UNC Single Crystal X-ray Facility report number c98. The unit cell parameters are provided in Table 1.

### 2.3. Differential scanning calorimetry (DSC)

A TA 2910S differential scanning calorimeter equipped with a data station (TA Instruments, New Castle, DE) was used to determine the thermal behavior of the GW275919X monohydrate. The temperature axis and the cell constant of the DSC cell were calibrated with indium. Sample (approximately 5 mg) in a crimped aluminum pan was heated at  $10^\circ\text{C}/\text{min}$  under a nitrogen purge at 40 mL/min.

### 2.4. Thermogravimetric analysis (TGA)

The TGA curves were obtained using a TA Hi-Res 2950 thermogravimetric analyzer linked to a data station (TA Instruments). The GW275919X monohydrate samples (10 mg) in open aluminum pans were heated at a rate of  $10^\circ\text{C}/\text{min}$  with a nitrogen purge at 60 mL/min.

### 2.5. Karl Fischer titrimetry (KFT)

The amount of water in the GW275919X monohydrate was determined using a Moisture Meter (Mitsubishi CA-05, Mitsubishi Chemical Industries Ltd., Tokyo, Japan). Sample was

weighed and quickly transferred to the titration vessel containing anhydrous methanol prior to titration.

### 2.6. Powder X-ray diffraction (PXRD)

The powder X-ray diffractometer and an “in-house” built environmental sample chamber have been previously described (Buckner et al., 1999). For the dehydration study, scans were collected at  $4^\circ 2\theta/\text{min}$  at a digital resolution of  $0.03^\circ 2\theta$  using copper  $K\alpha$  radiation while drying the covered sample at  $50^\circ\text{C}$  under a stream of dry nitrogen. The sample cover uses an X-ray transparent window. PXRD peak integration was performed by removing background and then integrating using the BACKGROUND and AREA programs, respectively, of Scintag’s DMS software, v. 3.35.

### 2.7. Polarized light microscopy

The GW275919X crystals before or after dehydration were observed under an optical microscope (M3J, Wild Heerbrugg, Heerbrugg, Switzerland) equipped with polarizer and an analyzer.

### 2.8. Hot stage microscopy (HSM)

The thermal events were observed on a hot stage (Mettler FP80, Mettler Instrument Corp., Highstown, NJ) under a microscope (M3J, Wild Heerbrugg), with photoautomat and a camera. A single crystal of GW275919X monohydrate was immersed in high boiling silicone oil (Aldrich Chemical Co., Milwaukee, WI) and heated at a rate of  $10^\circ\text{C}/\text{min}$ .

### 2.9. Molecular modeling

Single crystal structure data were imported into Cerius<sup>2</sup> (Molecular Simulations, Inc.) v.3.9 to provide visualization of the crystal structure, to construct molecular packing and hydrogen bonding diagram, and to calculate the simulated PXRD pattern. Morphology prediction was performed using the BFDH calculation.

Table 1  
Crystallographic data

Formula:  $\text{C}_{11}\text{H}_9\text{NOF}_2 \cdot \text{H}_2\text{O}$   
Crystal system: monoclinic  
Space group:  $P21/c$

#### Cell constants

$a$  (Å) = 14.3734  
 $b$  (Å) = 5.0336  
 $c$  (Å) = 15.4633  
 $\beta$  =  $105.11^\circ$   
Z value = 4

Calculated density = 1.397

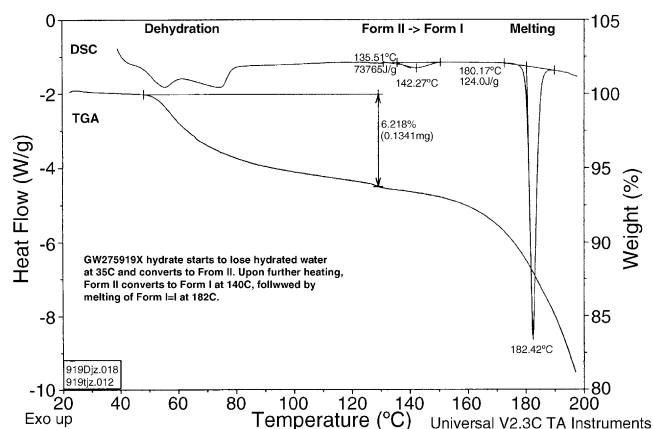


Fig. 2. DSC and TGA curves of GW275919 monohydrate.

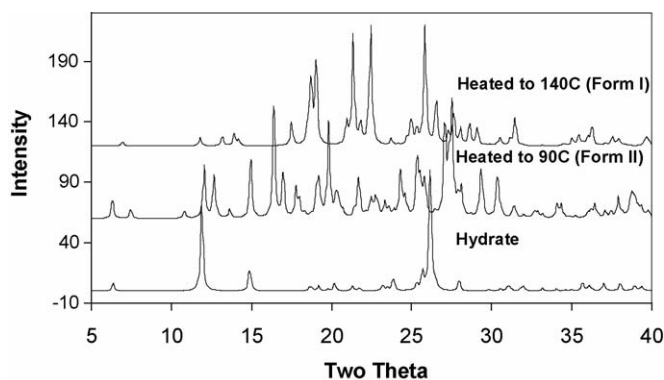


Fig. 3. Variable temperature PXRD of GW275919 monohydrate at room temperature, 90 °C and 140 °C.

### 3. Results and discussion

GW275919X exists in three anhydrous polymorphs (Forms I, II and III). The three polymorphs of GW275919X were previously characterized (Zhu and Sacchetti, 2001). Forms I and II, as well as Forms I and III, are enantiotropically related. Both Forms II and III convert to Form I at elevated temperatures through solid state phase transformation. The polymorphism and relationship among GW275919X crystal forms was subject of another publication.

The water stoichiometry of the GW275919X hydrate derived from Karl Fischer titrimetry suggested it is a monohydrate

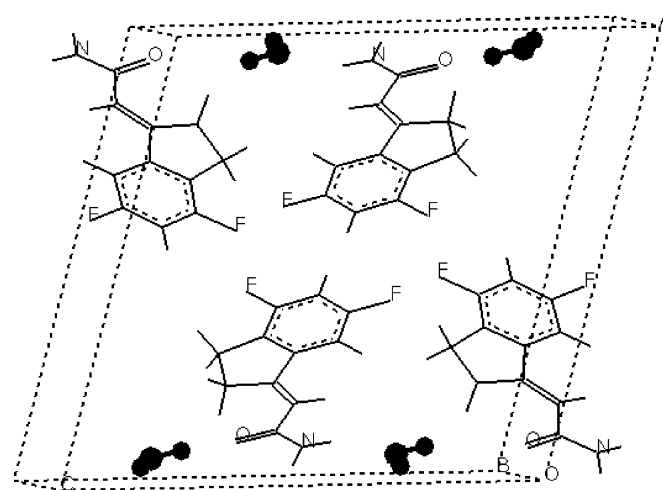


Fig. 5. Unit cells of the GW275919 monohydrate.

(6.3% (determined) versus 6.4% (calculated)). Confirmation of the monohydrate was also obtained by single crystal X-ray crystallography (Table 1). The DSC thermogram of the monohydrate shows four endotherms (Fig. 2). The first two broad and overlapping endotherms at the temperature ranging from 35 °C to 90 °C are associated with the dehydration. The sharp endotherm at 180 °C is associated with melting of polymorphic Form I. An endotherm at the temperature range 134–150 °C (Fig. 2) was also observed. With the aid of hot-stage PXRD (Fig. 3), the endotherm was determined to be a solid phase

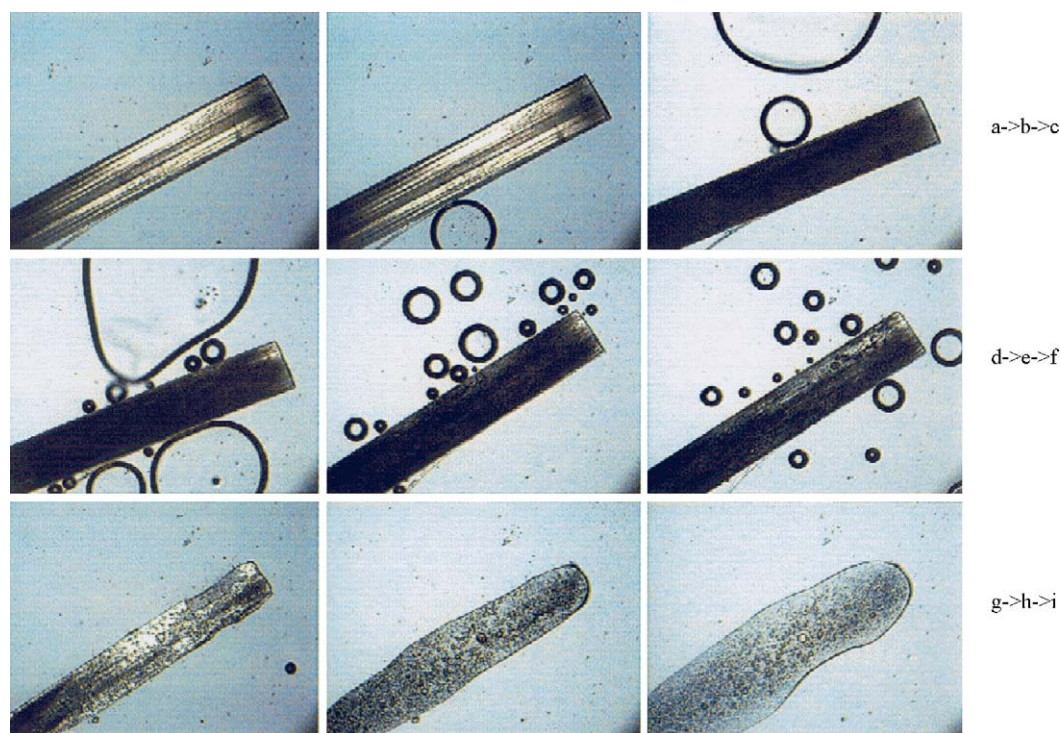


Fig. 4. Hot stage photomicrographs of GW275919 monohydrate at crystal at the following temperatures (°C) upon heating on a hot stage: (a) 30 (heating starts); (b) 45 (appearance of first bubble, dehydration takes place); (c) 51 (dehydration continues; crystal becomes dark); (d) 73 (highest rate of dehydration and dehydration completes); (e) 130 (bubbles due to sublimation); (f) 140 (solid state phase transition, Form II > Form I); (g) 150 (solid state phase transition completes); (h) 180.5 (Form I starts melting); (i) 182.3 (melting completes).

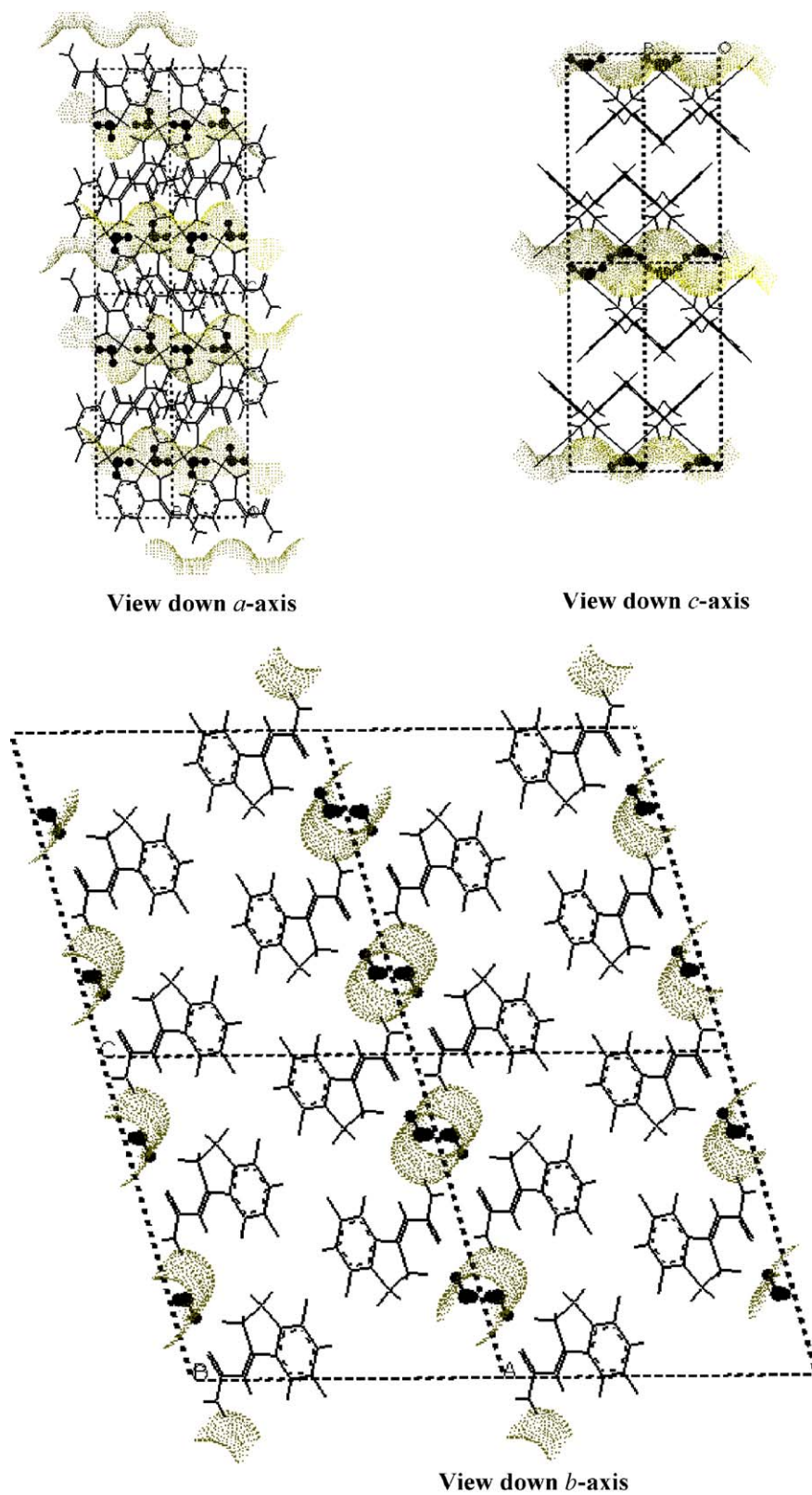


Fig. 6. Crystal packing diagrams of the GW275919X monohydrate. Looking down *a*- or *c*-axis, showing no water channel in either crystal direction. Looking down in *b*-axis, showing water tunnels parallel to this crystal axis.

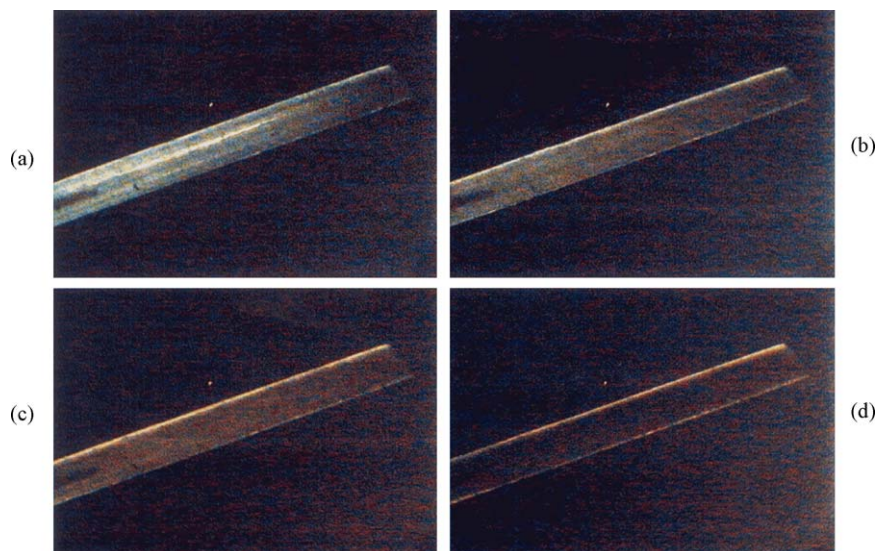


Fig. 7. Photomicrographs of GW275919X monohydrate crystal heated at 35 °C on a hot stage: (a) at start; (b) after 1 h; (c) after 2 h; (d) after 4 h.

transformation from Form II to I, followed by melting of Form I. TGA showed continuous weight loss due to initial dehydration (up to 130 °C) and subsequent sublimation (>130 °C). The sublimation was confirmed by TG–MS.

Upon heating the sample using environmental sample chamber (Buckner et al., 1999) to 90 °C in hot-stage PXRD, the monohydrate converts to the anhydrous polymorphic Form II. Upon further heating to 140 °C, the anhydrous Form II underwent solid state phase transformation to Form I (Fig. 3).

The changes in a single crystal of GW275919X monohydrate during the dehydration steps were observed under the hot-stage microscope (Fig. 4). The appearance of the bubbles actually began at 45 °C, from both the needle axis (*b*-axis) and the side of the crystal (*a*- or *c*-axis). The highest rate of dehydration occurs at 73 °C. Bubbles continue due to sublimation. Solid state transformation from Form II to I occurs

at 140 °C. On further heating to 180.5 °C, the Form I starts to melt.

Crystal structure data for GW275919X monohydrate are listed in Table 1. The unit cell is shown in Fig. 5. The crystal packing of the GW275919X monohydrate has tunnels filled with water molecules parallel to the *b*-axis (Fig. 6). Photomicrographs of the crystal, which was kept at 35 °C on hot stage, showed the dehydration was anisotropic and proceeded along the *b* crystal axis—the needle axis of the crystal (Fig. 7). The clear crystal becomes cloudy immediately upon heating and becomes darkened with the increase of time, corresponding to a phase transformation to the lower hydrate. The anisotropic behavior of crystals is explained by the preferential escape of the water molecules along these tunnels. Dehydration from other crystal directions would require the water molecules to penetrate the somewhat closely packed layers of nonpolar groups in the other two directions.

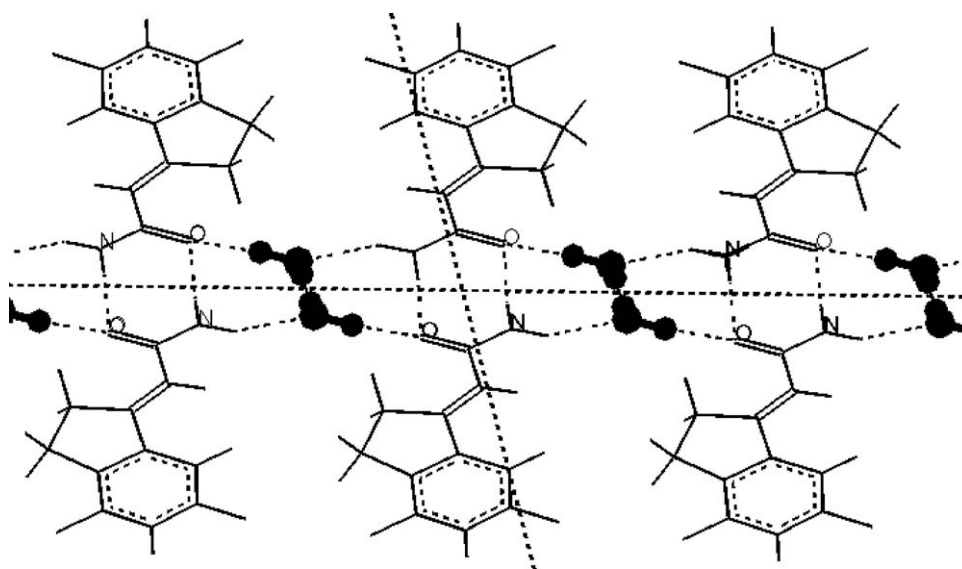


Fig. 8. H-bonding pattern of the GW275919X monohydrate.

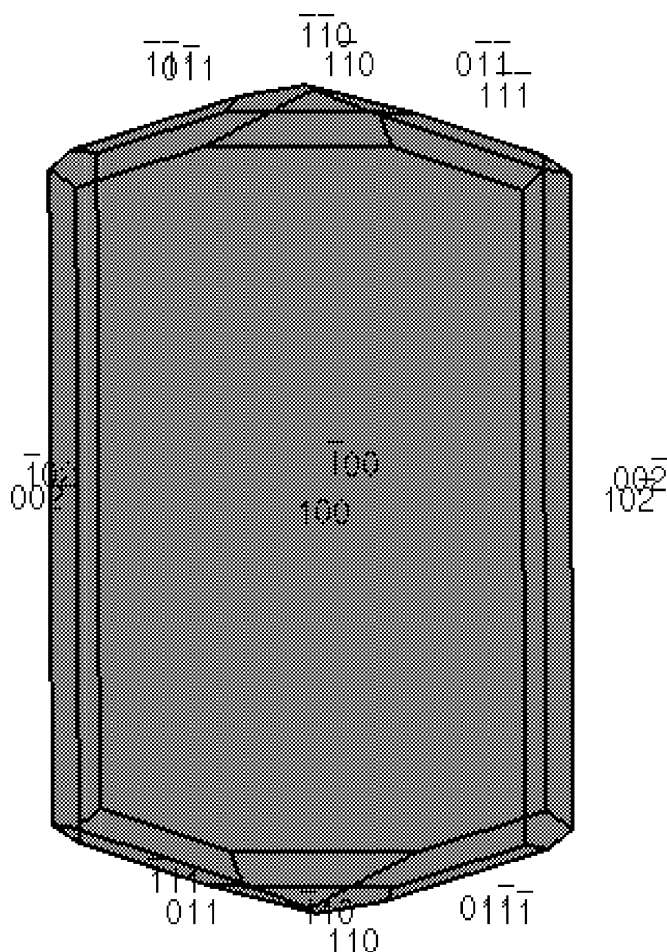


Fig. 9. Predicted crystal morphology of the GW275919 monohydrate.

A H-bonded chain is formed throughout the crystal structure (Fig. 8). The GW275919X monohydrate molecules are H-bonded to themselves via the amide groups and to water molecules. The amide groups and water molecules are fully saturated in H-bonds.

Morphology prediction was done using the BFDH calculation (Fig. 9). Note that the longest dimension of the predicted morphology is in the *b*-direction, which would correspond to the needle axis of the experimental crystals. Since water tunnels are along the *b*-axis, one would predict water loss at the ends of the needle, which is observed experimentally.

#### 4. Conclusions

GW275919X forms a monohydrate. Upon heating, the hydrate loses lattice water and converts to polymorphic Form

II. The Form II converts to Form I through solid state transformation upon further heating to 140 °C. Water molecules in the hydrate crystal of GW275919X involved hydrogen bonds and these hydrogen bonds contribute to the coherence of the crystal structure. A better understanding of the dehydration behavior and the crystal structure of the GW275919X monohydrate was achieved through the structure determination, molecular modeling and solid state characterization.

#### Acknowledgments

The author thanks Drs. Mark Sacchetti and Peter Varlashkin, Physical Properties Group, GlaxoSmithKline (Research Triangle Park, NC), for conducting molecular modeling work using Cerius<sup>2</sup> software and Dr. Peter White, Department of Chemistry, University of North Carolina at Chapel Hill, for determining the crystal structure of GW275919X.

#### References

- Agbada, O.C., York, P., 1994. Dehydration of theophylline monohydrate powder—effects of particle size and sample weight. *Int. J. Pharm.* 106, 33–40.
- Buckner, C., Kidd, C., Long, S., Varlashkin, P., Zhu, H., 1999. Environmentally controlled sample stage for Scintag's six-position XRD sample changer. *Powder Diffr.* 14, 296–299.
- Byrn, S.R., 1982. *Solid State Chemistry of Drugs*. Academic Press, New York, NY, pp. 59–74, 149–186.
- Forbes, R.T., York, P., Fawcett, V., Shields, L., 1992. Physicochemical properties of salts of *p*-aminosalicylic acid. I. Correlation of crystal structure and hydrate stability. *Pharm. Res.* 9, 1428–1435.
- Gabe, E.J., LePage, Y., Charland, J.P., Lee, F.L., White, P.S., 1989. NRCVAX, an interactive program system for structure analysis. *J. Appl. Crystallogr.* 22, 384–387.
- Hirsch, C.A., Messenger, R.J., Brannon, J.L., 1978. Fenoprofen: drug form selection and preformulation stability studies. *J. Pharm. Sci.* 67, 231–236.
- Ojala, W.H., Khankari, R.K., Grant, D.J.W., Gleason, W.B., 1996. Crystal structures and physical chemical properties of nedocromil zinc heptahydrate and nedocromil magnesium pentahydrate. *J. Chem. Cryst.* 26, 167–178.
- Zhu, H., Khankari, R.K., Padden, B.E., Munson, E.J., Gleason, W.B., Grant, D.J.W., 1996. Physicochemical characterization of nedocromil bivalent metal salt hydrates: 1. Nedocromil magnesium. *J. Pharm. Sci.* 85, 1026–1034.
- Zhu, H., Xu, J., Kidd, C., Long, S., Varlashkin, P., 2001a. Dehydration, hydration behavior and structural analysis of fenoprofen calcium. *J. Pharm. Sci.* 90, 845–859.
- Zhu, H., Varlashkin, P., Sacchetti, M., October 2001. Structural characterization and molecular modeling of GW275919 hydrate and solvates. In: 15th AAPS Annual Meeting, Denver, CO.
- Zhu, H., Sacchetti, M., October 2001. Polymorphism and crystal form selection of GW275919X. In: 15th AAPS Annual Meeting, Denver, CO.